Record warming in the South Pacific and western Antarctica associated with the strong central-Pacific El Niño in 2009–10

Tong Lee,[1] William R. Hobbs,[1] Joshua K. Willis,[1] Daria Halkides,[1] Ichiro Fukumori,[1] Edward M. Armstrong,[1] Akiko K. Hayashi,[1] W. Timothy Liu,[1] William Patzert,[1] and Ou Wang[1]

Received 27 July 2010; revised 19 August 2010; accepted 27 August 2010; published 14 October 2010.

[1] Satellite data for the past three decades reveal a record-high sea surface temperature (SST) anomaly within a large mid-latitude region of the south-central Pacific (SCP) during the mature phase of the 2009–10 El Niño, with a peak magnitude that is 5 times the standard deviation of local SST anomaly and is warmer than the concurrent tropical-Pacific SST anomaly. The SCP oceanic warming was confined to the upper 50 meters and is associated with an extreme and persistent anticyclone. Wind changes associated with the anticyclone caused the oceanic warming with surface heat flux and ocean processes playing equally important roles. The anticyclone diverted circumpolar westerlies and warm air towards Antarctica. Austral-summer SST in the Bellingshausen Sea also reached a three-decade high. The extreme atmospheric and oceanic anomalies in the South Pacific may have been fueled by the 2009–10 El Niño because of its record-high SST anomaly in the central-equatorial Pacific. **Citation:** Lee, T., W. R. Hobbs, J. K. Willis, D. Halkides, I. Fukumori, E. M. Armstrong, A. K. Hayashi, W. T. Liu, W. Patzert, and O. Wang (2010), Record warming in the South Pacific and western Antarctica associated with the strong central-Pacific El Niño in 2009–10, *Geophys. Res. Lett.*, *37*, L19704, doi:10.1029/2010GL044865.

1. Introduction

[2] Generally speaking, interannual anomalies (the deviation from a seasonal climatology) of SST in the extra-tropical South Pacific are smaller than those in the tropical Pacific associated with El Niño-Southern Oscillation (ENSO). However, during late 2009 and early 2010 (austral spring and summer), a large SST anomaly developed in the south-central Pacific (SCP) over a region approximately the size of the continental United States, and with a magnitude exceeding the SST anomaly in the tropical Pacific associated with the concurrent El Niño (Figure 1) by more than 0.5°C.

[3] The extra-tropical climate in the South Pacific sector is known to be influenced both by ENSO and the Southern Annular Mode (SAM). ENSO is associated with variations in large-scale zonal gradients of atmospheric pressure and sea surface temperature (SST) in the tropical Pacific [e.g., *McPhaden et al.*, 2006] due to ocean-atmosphere interactions, and it is the dominant mode of interannual climate variability originating in the tropical Pacific. The SAM, which reflects the non-seasonal meridional difference in air pressure between subpolar and mid-latitude regions, is primarily due to atmospheric internal dynamics [*Thompson and Wallace*, 2000] but it is modulated by ocean-atmosphere coupling [*Sen Gupta and England*, 2007].

[4] Here we use a suite of satellite and in-situ observations, as well as an atmospheric reanalysis product to document the oceanic and atmospheric conditions associated with the SCP anomaly and to examine their relationships with ENSO and SAM. The data and methods used for the analysis are described in section 2. The results of the analysis are presented in section 3. A summary of the findings and their broader implications are provided in section 4.

2. Data and Methods

2.1. Oceanic Data

[5] The primary ocean datasets used in this analysis are: (1) Reynolds's ¼° Group for High Resolution SST (GHRSST) Level 4 AVHRR OI daily SST product for the period of 1982 to July 2010 [*Reynolds et al.*, 2007] (available from http://ghrsst.jpl.nasa.gov and http://ghrsst.nodc.noaa.gov); the product is based on measurements from Advanced Very High Resolution Radiometers (AVHRR) calibrated by (and blended with) in-situ observations. (2) vertical profiles of ocean temperature measured by Argo floats from mid 2004 to February 2010. Auxiliary in-situ observations of SST from buoys, drifters, and ship-board measurements (obtained from the FNMOC GODAE server, http://www.usgodae.org) were also used to examine the accuracy of the GHRSST product in describing the SCP warming.

2.2. Atmospheric Data

[6] The description of the atmospheric variability was based on different variables obtained from the National Center for Environmental Prediction (NCEP) and Department of Energy (DOE) reanalysis II product that covers the period of 1979–2009 [*Kanamitsu et al.*, 2002] (referred to as the NCEP product hereafter). The SAM index [*Marshall*, 2003] was obtained from http://www.nerc-as.ac.uk/icd/gjma/sam.html. Auxiliary satellite observations were used to evaluate the NCEP product. These satellite observations include (1) ocean surface wind speed observations during 2002 to February 2010 obtained from the JASON-1 altimeter launched by the National Aeronautic and Space Administration (NASA) (processed by the Jet Propulsion Laboratory) and (2) ocean surface vector wind measurements from the ASCAT scatterometer on board of the MetOp satellite launched by European's Space Agency from March 2007 to February 2010,

[1]Jet Propulsion Laboratory, California Institute of Technology, Pasadena, California, USA.

0094-8276/10/2010GL044865

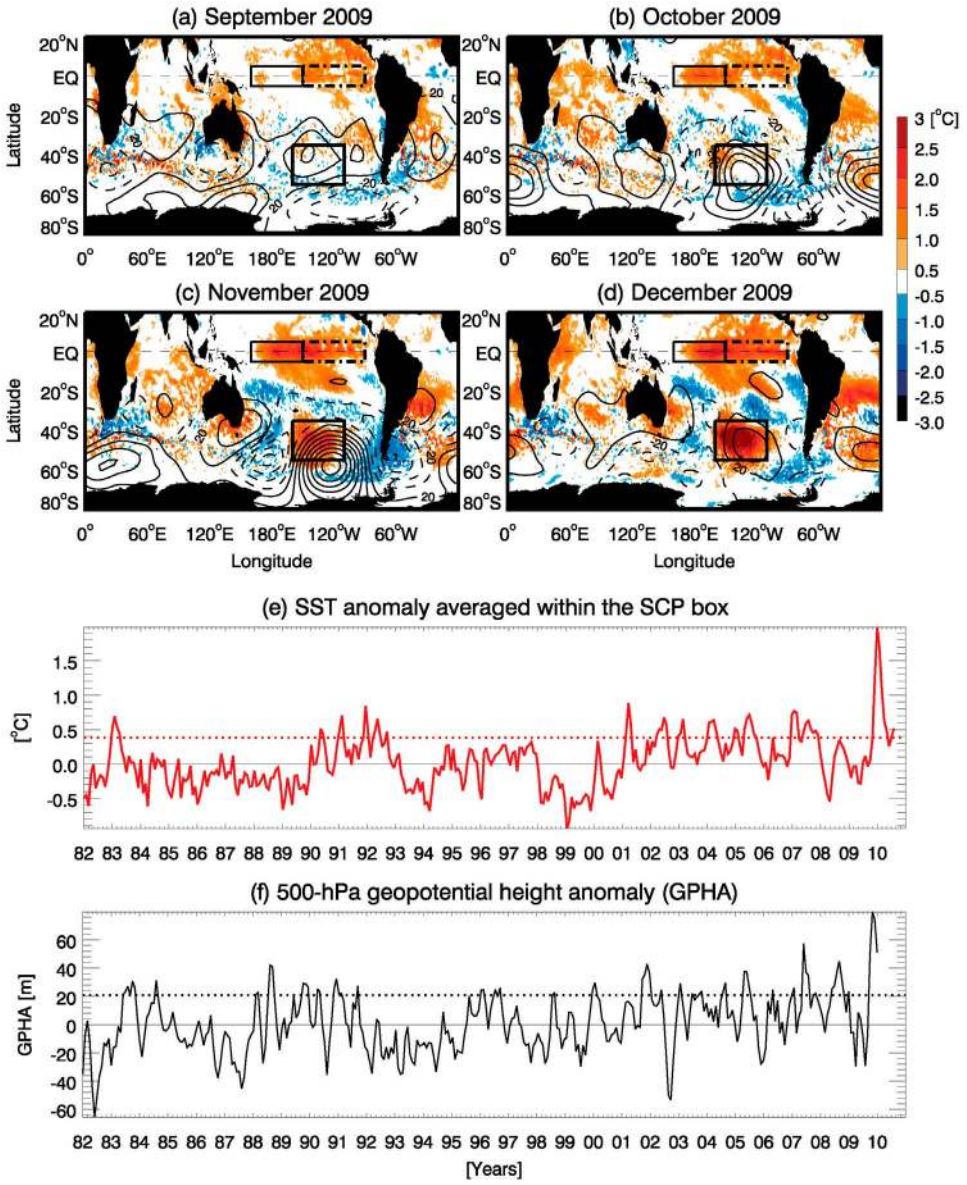

Figure 1. (a–d) SST anomaly (colors) and 500-hPa geopotential height anomaly (contours, increment is 40 m). The box in the South Pacific indicates the SCP region (160–110°W, 55–35°S).The two boxes in the tropics represent the Niño4 (150°–90°W, 5°S–5°N, solid line) and Niño3 (170°–120°W, 5°S–5°N, dashed-dotted line) regions. (e) Time series of SST anomaly and (f) 500-hPa geopotential height anomaly averaged within the SCP box. The dashed lines in Figures 1e and 1f represent the level of one standard deviation for the respective time series.

available from the Physical Oceanography Distributed Active Archive Center (PO.DAAC, http://podaac.jpl.nasa.gov).

[7] The GHRSST data were used to describe the evolution of the SCP warming and its relationship to the concurrent El Niño event. Argo float data were used to determine the vertical extent of the SCP warming. The NCEP and satellite wind products were used to characterize the atmospheric conditions associated with SCP warming. The atmospheric and oceanic data were used to evaluate the role of surface heat flux and ocean processes in causing the SCP warming.

3. Results

[8] Figures 1a–1d shows the SST anomaly (referenced to the 1982–2008 seasonal climatology) in late 2009. Anomalous warming in the SCP region began to emerge in September and developed rapidly in November and December. By December, the SST anomaly averaged within the SCP box (160–110°W, 55–35°S) reached a record high for the past three decades, with a peak magnitude of approximately 2°C (Figure 1e). This is over 5 times of the standard deviation of the monthly SCP SST anomaly (0.38°C). In-situ measurements from buoys, drifters, and ship-board observations confirm that potential errors in the GHRSST are negligible: the mean difference between the GHRSST and the in-situ SST averaged within the SCP box is only 0.08°C in December 2009 and −0.03°C in January 2010 (the mature phase of the SCP warming event). Argo float measurements near the surface show comparable warming to the satellite

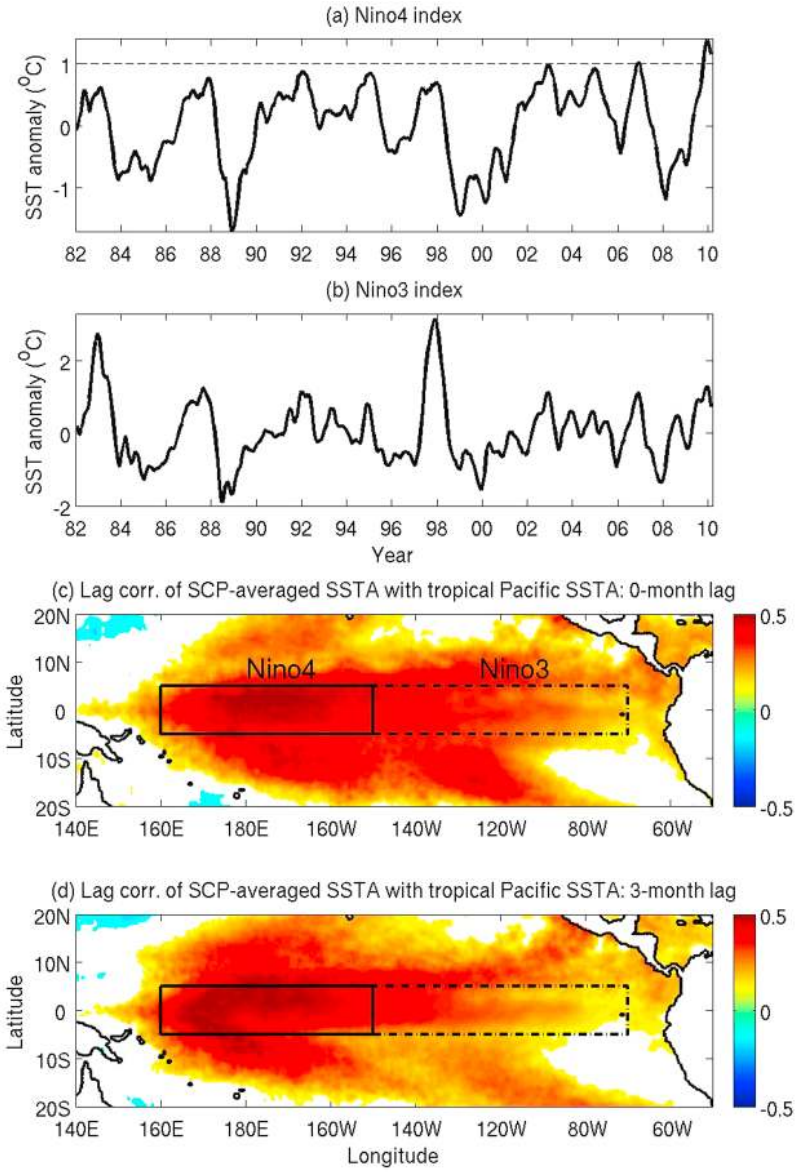

Figure 2. Three-month smoothed (a) Niño4 index (SST anomaly averaged within Niño4) and (b) Niño3 index (SST anomaly averaged within Niño3). Lag correlation of SCP-averaged SST anomaly with SST anomalies in the tropical Pacific for (c) zero-month and (d) three-month lag. Values not significantly different from zero at the 95% confidence level are masked.

SST (Figure S1 of the auxiliary material).[1] Vertical profiles of ocean temperature reveal that the warming was confined to the upper 50 m, the approximate mixed-layer depth in the region during austral spring-summer (Figure S1). The SCP warming event decayed substantially in the first four months of 2010 (Figure S2).

[9] The SCP warming lagged the early development of the 2009–10 El Niño, but it peaked in December when the El Niño reached its peak (as shown by the Niño4 and Niño3 indices in Figures 2a–2b; the Niño4 and Niño3 boxes were shown both in Figures 1 and 2). At this time (during austral spring-summer) the mixed-layer is relatively shallow, so the response of southern-hemisphere SST to El Niño tends to be large. This raises the question of whether the El Niño may have fueled the SCP warming. Although the Niño3 index of the 2009–10 El Niño is much smaller than those of the 1982–83 and 1997–98 events (Figure 2b), its Niño4 index is the largest for the past three decades (Figure 2a). In fact, the peak Niño4 index associated with the 2009–10 El Niño, approximately 1.4°C, is more than 60% larger than the averaged value of peak Niño4 indices for other El Niño events in the past three decades.

[10] To analyze the possibility of a relationship between the SCP warming and El Niño, the correlations between the SCP-averaged SST anomaly with SST anomalies in the tropical Pacific for the entire period (1982–2010) are presented in Figures 2c–2d with the SCP SST lagged by 0 and 3 months, respectively. The SCP SST anomaly is much better correlated with SST anomalies in the central-equatorial

[1]Auxiliary materials are available in the HTML. doi:10.1029/2010GL044865.

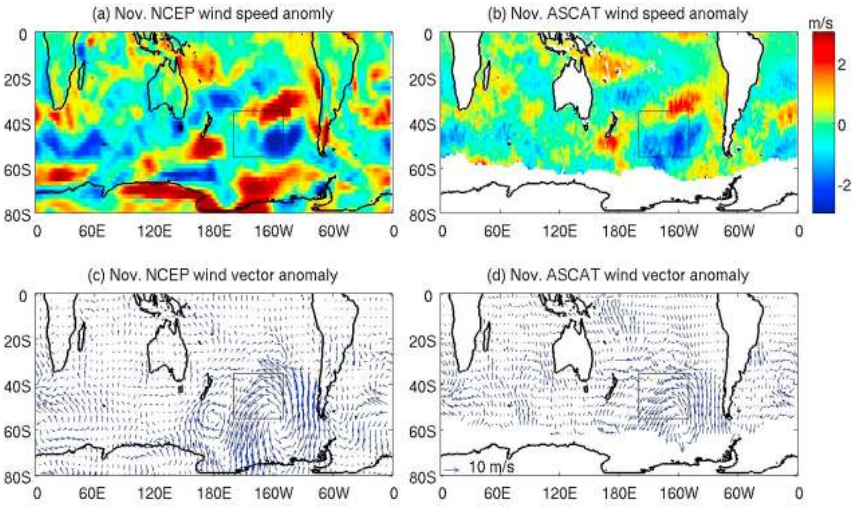

Figure 3. November 2009 anomaly of (a and b) wind speed and (c and d) wind vector from NCEP (Figures 3a and 3c) and ASCAT (Figures 3b and 3d). The anomalies for NCEP are referenced to the 1982–2008 seasonal climatology. Those for ASCAT are referenced to the March 2007–February 2010 "seasonal climatology".

Pacific (CP) (the Niño4 box) than with those in the eastern-equatorial Pacific (EP) (the Niño3 box), especially with the SCP lagging. The better lag-correlation of SCP SST with Niño4 SST and the record high Niño4 SST associated with the 2009–10 El Niño suggest that it may have contributed to the record SCP warming. Such relationship is also consistent with the fact that El Niño events that have large SST anomalies in the EP region (e.g., the 1982–83, 1986–87, and 1997–98 events) do not correspond to large SCP warming. EP-El Niño events tend to have relatively small SST anomalies in the Niño4 region. However, lag correlation does not necessarily reflect a causal relation. Further study is needed to examine if the 2009–10 CP-El Niño has amplified the SCP SST anomaly.

[11] The SCP oceanic warming coincided with an extreme atmospheric high-pressure system (referred to hereafter as an anticyclone), illustrated in Figure 1 by solid contours representing the NCEP 500-hPa geopotential height anomaly (GPHA) (referenced to the 1982–2008 seasonal climatology). This anticyclone emerged in September, strengthened during October–November, and decayed in December. The anticyclone was extremely strong. In November 2009, the 500-hPa GPHA averaged within the SCP box reached its highest value since 1982 (Figure 1f). Persistent anticyclones are common in the southwest and southeast Pacific, but are relatively unusual in the SCP region [*Sinclair*, 1996; *Hobbs and Raphael*, 2010]. A survey of anticyclones in the SCP region since 1982 indicates that these events typically last for a month, with only 20% of the events lasting 2 months or more.

[12] The importance of the SAM to southern-hemisphere climate makes it necessary to consider its potential relationship to the anticyclone. A negative value of the SAM index is associated with weaker zonal winds and stronger zonal asymmetry (more high- and low-pressure centers zonally). The SAM index was negative during July–August 2009 (Figure S3), which may be related to the weak anticyclone in the SCP in September 2009 (Figure 1a). However, there is little anomaly in the SAM during October–December when the anticyclone was the strongest, indicating that SAM did not play a role in strengthening the anticyclone later in the year.

[13] To investigate the potential relationship between SCP anticyclones and SST anomalies in the eastern- and central-equatorial Pacific, we examined the Niño4 and Niño 3 SST indices for the months with and without a significant anticyclone. The record shows that SCP anticyclones tend to occur when the Niño 4 index is positive and the Niño3 index is negative. El Niño events are associated with enhanced tropical convection due to warm tropical SST anomalies. The resultant pressure anomalies can spread to the South Pacific via either an atmospheric Rossby wave train (known as the Pacific-South American or PSA mode) or through the modification of mid-latitude meridional mean circulation [e.g., *Mo*, 2000; *Houseago-Stokes and McGregor*, 2000; *Turner*, 2004; *Yuan*, 2004]. The strengthening of the SCP anticyclone in late 2009 is probably caused in part by the record-high SST anomaly in the CP region. Again, a statistical relation does not necessarily indicate a causal relationship. Further investigation is necessary to study the physics through which central-Pacific warming affects SCP anticyclones.

[14] Persistent anticyclones are associated with blocking of atmospheric flows, and a consequent decrease in wind speed due to the reduction of synoptic storms within the pressure anomaly. The monthly means of daily averaged wind speed anomaly indicate an abrupt drop in wind speed in late 2009 (Figure S4a) due to a reduction in synoptic variability (sub-weekly wind fluctuations) (Figure S4b). November-averaged daily wind speed anomaly shows that much of the wind-speed reduction (indicated by negative values in Figure 3a) occurred in the southeastern part of the SCP box towards the center of the anticyclone. The vector wind anomaly associated with the strong anticyclone (Figure 3c) shows an easterly anomaly (i.e., weaker westerly winds) in the SCP box. Further south, the wind anomaly reached all the way to Antarctica. The reduction of wind speed and the spatial structure of the wind anomaly associated with the SCP anticyclone in late 2009 are represented consistently in both the NCEP product (Figures 3a and 3c)

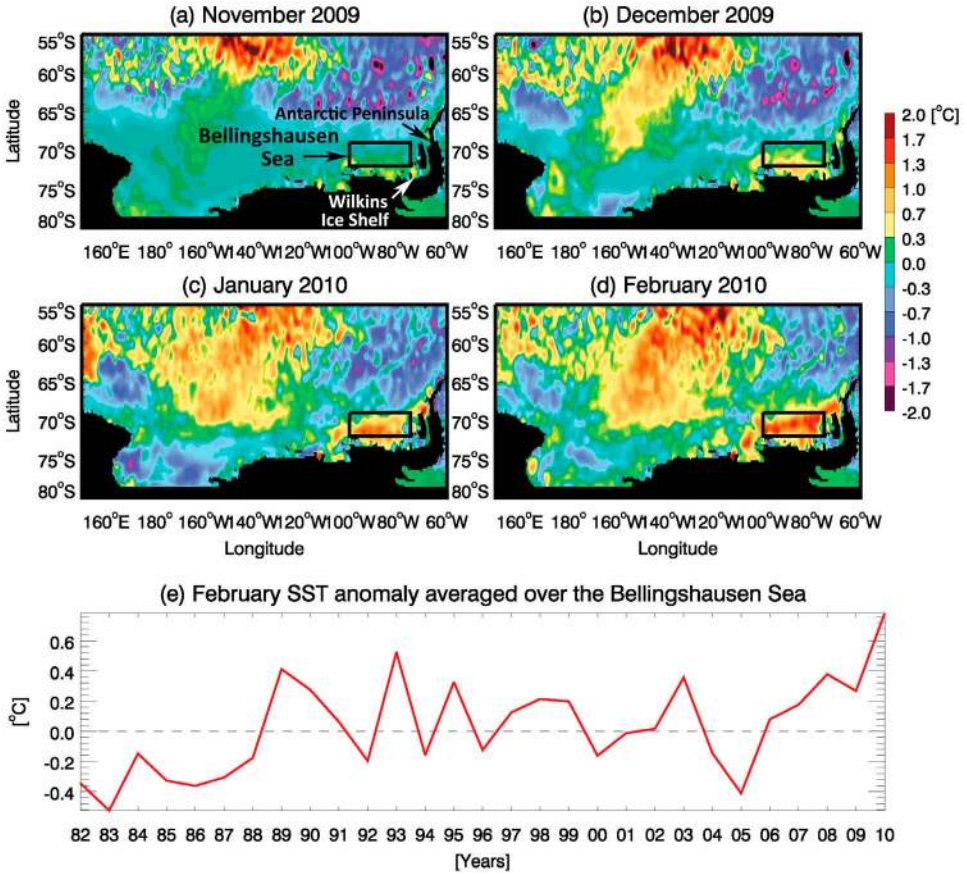

Figure 4. (a–d) SST anomaly near the Bellingshausen Sea associated with the South Pacific warming. (e) Austral-summer (February) SST anomaly averaged over the Bellingshausen Sea (100°–75°W, 69°–72°S).

and the ASCAT measurements (Figures 3b and 3d). The relatively abrupt reduction of wind speed from November 2008 to November 2009 (Figure S4) is approximately 20% for the NCEP product as well as for the ASCAT and JASON-1 wind observations.

[15] The anomalously low wind speed and the easterly wind anomaly in the SCP region worked in tandem to produce the oceanic warming. The low wind speed resulted in reduced latent and sensible heat loss, which caused anomalous oceanic warming (Table S1). Meanwhile, the easterly wind anomaly drove anomalous southward ocean surface current (i.e., meridional Ekman flow), which weakened the normal northward advection of colder waters from the south to re-enforced the SCP warming. These two effects were estimated to have comparable contributions with each accounting for about 40% of the oceanic warming (see auxiliary material). This is qualitatively consistent with previous studies of mixed-layer temperature balance in the region [*Verdy et al.*, 2006; *Vivier et al.*, 2010]. Additional (subsurface) ocean processes associated with weaker mechanical stirring by the wind are also expected to have contributed to the warming.

[16] The anticyclone (e.g., Figures 3c–3d) deflected the circumpolar westerly winds southward, bringing warmer mid-latitude air to high-latitude Southern Ocean and Antarctica. Ocean currents also help spread the anomalous ocean warming on longer time scales [*Peterson and White*, 1998]. A tongue of positive SST anomaly extending towards the Ross Sea and a warming in the western Antarctic Peninsula near the Bellingshausen Sea (Figures 4a–4d) were associated with the anomalous SCP event. These regions are known to be affected by ENSO with lag times of a few months or longer [*Turner*, 2004; *Yuan*, 2004]. The average SST anomaly in the Bellingshausen Sea increased from October 2009 to February 2010, also reaching a record summertime high for the past three decades (Figure 4e). The warming extended all the way into the region of the Wilkins ice shelf, which partially disintegrated in 2008 [*Humbert and Braun*, 2008].

4. Concluding Remarks

[17] A suite of satellite and in-situ data have been used to document the atmospheric and oceanic conditions associated with a record warming event in the SCP region and western Antarctica during austral spring-summer associated with the 2009–10 El Niño. The magnitude of the SST anomaly associated with the SCP warming is 5 times the standard deviation of local SST anomaly and is larger than the SST anomaly in the tropical Pacific associated with the concurrent El Niño event. The SCP warming is confined to the upper 50 meters of the ocean and is associated with an extreme and persistent anticyclone. Wind changes associated with the anticyclone cause the oceanic warming primarily through reduced latent and sensible (oceanic) heat loss and by weaker advection of cold waters from the south. The surface heat flux and ocean processes have comparable contributions. The anticyclone diverted the circumpolar westerly wind and the warm mid-latitude air that it carried

southward towards western Antarctica. Austral-summer SST in the Bellingshausen Sea and near the unstable Wilkins ice shelf also reached a three-decade high.

[18] Circumstantial evidence suggests that the strong CP-El Niño in 2009–2010 may have amplified the event in SCP and western Antarctica. In the past two decades, a new type of El Niño having maximum warming in the CP region has become more common while the classical type of El Niño having maximum warming in the eastern-equatorial Pacific (EP) has become less common [e.g., *Ashok et al.*, 2007; *Kao and Yu*, 2009]. A recent study suggests that the occurrence ratio of CP-El Niño versus EP-El Niño may become as large as five under the projected global warming scenarios [*Yeh et al.*, 2009]. The intensity of El Niño in the CP region has doubled in the past three decades, with the 2009–10 event being the strongest CP-El Niño observed to date [*Lee and McPhaden*, 2010]. Extreme warming events like the one documented here in the SCP region and western Antarctica may adversely affect the delicate balance of the ocean-ice-atmosphere system of the Antarctic environment, especially if they become more common in the future.

[19] **Acknowledgments.** The research described in this paper was in part carried out at the Jet Propulsion Laboratory, California Institute of Technology, under a contract with NASA, with supports from NASA Physical Oceanography and EOSDIS programs. Government sponsorship acknowledged. This research was motivated by PO.DAAC's El Niño animation and an initial discussion of the SCP SST with Bob Leben of the University of Colorado.

References

Ashok, K., S. K. Behera, S. A. Rao, H. Weng, and T. Yamagata (2007), El Niño Modoki and its possible teleconnection, *J. Geophys. Res.*, *112*, C11007, doi:10.1029/2006JC003798.

Hobbs, W. R., and M. N. Raphael (2010), Characterizing the zonally asymmetric component of the SH circulation, *Clim. Dyn.*, doi:10.1007/s00382-009-0663-z, in press.

Houseago-Stokes, R. E., and G. R. McGregor (2000), Spatial and temporal patterns linking southern low and high latitudes during South Pacific warm and cold events, *Int. J. Climatol.*, *20*, 793–801, doi:10.1002/1097-0088(20000615)20:7<793::AID-JOC502>3.0.CO;2-9.

Humbert, A., and M. Braun (2008), The Wilkins ice shelf, Antarctica: Break-up along failure zones, *J. Glaciol.*, *54*, 943–944, doi:10.3189/002214308787780012.

Kanamitsu, M., W. Ebisuzaki, J. Woollen, S.-K. Yang, J. J. Hnilo, M. Fiorino, and G. L. Potter (2002), NCEP-DEO AMIP-II Reanalysis (R-2), *Bull. Am. Meteorol. Soc.*, *83*, 1631–1643.

Kao, H.-Y., and J.-Y. Yu (2009), Contrasting eastern-Pacific and central-Pacific types of ENSO, *J. Clim.*, *22*, 615–632, doi:10.1175/2008JCLI2309.1.

Lee, T., and M. J. McPhaden (2010), Increasing intensity of El Niño in the central-equatorial Pacific, *Geophys. Res. Lett.*, *37*, L14603, doi:10.1029/2010GL044007.

Marshall, G. J. (2003), Trends in the Southern Annular Mode from observations and reanalyses, *J. Clim.*, *16*, 4134–4143, doi:10.1175/1520-0442(2003)016<4134:TITSAM>2.0.CO;2.

McPhaden, M. J., S. E. Zebiak, and M. H. Glantz (2006), ENSO as an integrating concept in Earth science, *Science*, *314*, 1740–1745, doi:10.1126/science.1132588.

Mo, K. C. (2000), Relationships between low-frequency variability in the Southern Hemisphere and sea surface temperature anomalies, *J. Clim.*, *13*, 3599–3610, doi:10.1175/1520-0442(2000)013<3599:RBLFVI>2.0.CO;2.

Peterson, R. G., and W. B. White (1998), Slow oceanic teleconnections linking the Antarctic circumpolar wave with the tropical El Niño–Southern Oscillation, *J. Geophys. Res.*, *103*, 24,573–24,583.

Reynolds, R. W., T. M. Smith, C. Liu, D. B. Chelton, K. Casey, and M. G. Schlax (2007), Daily high-resolution-blended analyses for sea surface temperature, *J. Clim.*, *20*, 5473–5496, doi:10.1175/2007JCLI1824.1.

Sen Gupta, A., and M. H. England (2007), Coupled ocean-atmosphere feedback in the Southern Annular Mode, *J. Clim.*, *20*, 3677–3692, doi:10.1175/JCLI4200.1.

Sinclair, M. R. (1996), A climatology of anticyclones and blocking for the Southern Hemisphere, *Mon. Weather Rev.*, *124*, 245–263, doi:10.1175/1520-0493(1996)124<0245:ACOAAB>2.0.CO;2.

Thompson, D. W. J., and J. M. Wallace (2000), Annular modes in the extratropical circulation. Part I: Month-to-month variability, *J. Clim.*, *13*, 1000–1016, doi:10.1175/1520-0442(2000)013<1000:AMITEC>2.0.CO;2.

Turner, J. (2004), The El Niño-Southern Oscillation and Antarctica, *Int. J. Climatol.*, *24*, 1–31, doi:10.1002/joc.965.

Verdy, A., J. Marshall, and A. Czaja (2006), Sea surface temperature variability along the path of the Antarctic circumpolar current, *J. Phys. Oceanogr.*, *36*, 1317–1331, doi:10.1175/JPO2913.1.

Vivier, F., D. Iudicore, F. Busdraghi, and Y.-H. Park (2010), Dynamics of sea-surface temperature anomalies in the Southern Ocean diagnosed from a 2D mixed-layer model, *Clim. Dyn.*, *34*, 153–184, doi:10.1007/s00382-009-0724-3.

Yeh, S.-W., J.-S. Kug, B. Dewitte, M.-H. Kwon, B. Kirtman, and F.-F. Jin (2009), El Niño in a changing climate, *Nature*, *461*, 511–514, doi:10.1038/nature08316.

Yuan, X. (2004), ENSO-related impacts on Antarctic sea ice: A synthesis of phenomenon and mechanisms, *Antarct. Sci.*, *16*, 415–425, doi:10.1017/S0954102004002238.

E. M. Armstrong, I. Fukumori, D. Halkides, A. K. Hayashi, W. R. Hobbs, T. Lee, W. T. Liu, W. Patzert, O. Wang, and J. K. Willis, Jet Propulsion Laboratory, California Institute of Technology, 4800 Oak Grove Dr., Pasadena, CA 91109, USA. (Tong.Lee@jpl.nasa.gov)